



Published as: *Cell Host Microbe*. 2012 August 16; 12(2): 166–176.

## The *Legionella pneumophila* EnhC protein interferes with immunestimulatory muramyl peptide production to evade innate immunity

Mingyu Liu<sup>2,3,§</sup>, Eva Haenssler<sup>1,2</sup>, Tsuyoshi Uehara<sup>2,\*</sup>, Vicki P. Losick<sup>2,3,a</sup>, James T. Park<sup>2</sup>, and Ralph R. Isberg<sup>1,2,4</sup>

<sup>1</sup>Howard Hughes Medical Institute Tufts University School of Medicine, Boston, MA 02115, USA

<sup>2</sup>Department of Molecular Biology and Microbiology Tufts University School of Medicine, Boston, MA 02115, USA

<sup>3</sup>Graduate Program in Molecular Microbiology, Sackler School of Graduate Biomedical Science Tufts University School of Medicine, Boston, MA 02115, USA

### Abstract

Successful pathogens have evolved to evade innate immune recognition of microbial molecules by pattern recognition receptors (PRR), which control microbial growth in host tissues. Upon *Legionella pneumophila* infection of macrophages, the cytosolic PRR Nod1 recognizes anhydro-disaccharide-tetrapeptide (anhDSTP) generated by soluble lytic transglycosylase (SltL), the predominant bacterial peptidoglycan degrading enzyme, to activate NF- $\kappa$ B-dependent innate immune responses. We show that *L. pneumophila* periplasmic protein EnhC, which is uniquely required for bacterial replication within macrophages, interferes with SltL, to lower anhDSTP production. *L. pneumophila* mutant strains lacking EnhC ( $\Delta$ enhC) increase Nod1-dependent NF- $\kappa$ B activation in host cells, while reducing SltL activity in a  $\Delta$ enhC strain restores intracellular bacterial growth. Further, *L. pneumophila* $\Delta$ enhC is specifically rescued in Nod1-, but not Nod2-, deficient macrophages, arguing that EnhC facilitates evasion from Nod1 recognition. These results indicate that a bacterial pathogen regulates peptidoglycan degradation to control the production of PRR ligands and evade innate immune recognition.

### Introduction

The Gram-negative intracellular bacterium *Legionella pneumophila* is the causative agent of Legionnaires' disease (Fraser et al. 1977; McDade et al. 1977). Fresh water amoebae, which support *L. pneumophila* intracellular replication, form a natural bacterial reservoir that is thought to result in selective pressure for traits contributing to virulence in the human host (Rowbotham 1980). Disease is caused by inhalation of aerosols from fresh water supplies followed by ingestion of the bacteria by alveolar macrophages (McDade et al. 1977). Within all cell types, *L. pneumophila* resides and replicates in a membrane-bound compartment

© 2013 Elsevier Inc. All rights reserved.

<sup>4</sup>Corresponding Author ralph.isberg@tufts.edu.

<sup>§</sup>Current address: Infection Discovery Bioscience, AstraZeneca R&D, Waltham, MA 02451

<sup>\*</sup>Current address: Novartis Institutes for Biomedical Research, 4560 Horton St., Emeryville, CA 94608

<sup>a</sup>Current address: Department of Embryology, Carnegie Institution for Science, Baltimore, MD 21218

**Publisher's Disclaimer:** This is a PDF file of an unedited manuscript that has been accepted for publication. As a service to our customers we are providing this early version of the manuscript. The manuscript will undergo copyediting, typesetting, and review of the resulting proof before it is published in its final citable form. Please note that during the production process errors may be discovered which could affect the content, and all legal disclaimers that apply to the journal pertain.

surrounded by endoplasmic reticulum (ER), called the *Legionella* containing vacuole (LCV) (Horwitz 1983; Swanson and Isberg 1995; Kagan and Roy 2002). The *L. pneumophila* Icm/Dot Type IV protein system is required for formation of the LCV (Berger and Isberg 1993; Segal and Shuman 1997; Segal et al. 1998; Vogel et al. 1998). Over 200 different protein substrates have been identified as having recognition sequences that allow translocation into host cells via the Icm/Dot system (Luo and Isberg 2004; de Felipe et al. 2005; Burstein et al. 2009; Huang et al. 2010).

As most of the selective pressures that gave rise to the pathogenic potential of *L. pneumophila* resulted from growth within amoebae, *L. pneumophila* should not express a cadre of proteins specific for survival in macrophages (Rowbotham 1980). The *L. pneumophila* periplasmic protein EnhC appears to be an exception to this rule (Liu et al. 2008). A *L. pneumophila*  $\Delta$ enhC strain is selectively restricted by macrophages previously exposed to bacteria, as the mutant grows with wild type kinetics in the amoebal *Dictyostelium discoideum* species (Liu et al. 2008). Possibly related to this observation, the absence of EnhC results in a compromised bacterial envelope, which may allow selective sensitivity to cytokine-stimulated macrophages (Liu et al. 2008).

Innate immune recognitions of microorganisms by membrane bound Toll-like receptors (TLR) and cytosolic Nod-like receptors (NLR) are primary strategies for controlling pathogens (Roy and Mocarski 2007; Ishii et al. 2008). At least three classes receptors are involved in recognition and restriction of *L. pneumophila* in both cultured macrophages and mouse infection models (Archer and Roy 2006; Hawn et al. 2006; Archer et al. 2009; Archer et al. 2010). Intracellular replication of *L. pneumophila* is restricted in macrophages from C57BL/6 mice, due to coordinate recognition of *L. pneumophila* flagellin by NLR sensors Naip5/Birc1e and Ipaf (Nlrc4/Card12) (Amer et al. 2006; Molofsky et al. 2006; Ren et al. 2006; Zamboni et al. 2006; Lightfield et al. 2008). In addition, Rip2 and MyD88, critical components of peptidoglycan (PG)-dependent Nod signaling and TLR signaling respectively, modulate host cell responses to *L. pneumophila* via NF- $\kappa$ B (Losick and Isberg 2006; Shin et al. 2008; Bartfeld et al. 2009). Mice defective for MyD88 function are further impaired for restriction of *L. pneumophila* if they lack either the Rip2-dependent signaling or the Naip5/Ipaf signaling, indicating that cytosolic flagellin and PG recognition synergize with TLR signaling to allow innate immune clearing of *L. pneumophila* in mice (Archer et al. 2010). Therefore, the ability of *L. pneumophila* to modulate production of bacterial products that stimulate pattern recognition should alter host cell recognition of the microorganism.

Soluble lytic murein transglycosylase (Slt), the predominant enzyme involved in PG degradation, generates *N*-acetylglucosamine (GlcNAc)-1,6-anhydro-*N*-acetylmuramic acid (MurNAc)-peptide (G-anhM-peptide) by cleaving the glycosidic bond between MurNAc and GlcNAc (Holtje 1996; Park and Uehara 2008). Slt activity generates pores for insertion of newly synthesized PG fragments or protein complexes, facilitating bacterial growth and division. The action of all PG degradation enzymes must be strictly regulated to maintain a critical balance between PG synthesis and degradation (Scheurwater et al. 2008). The mammalian Nod1 protein, one of the archetypal NLR proteins, recognizes the G-anhM-peptide generated by Slt (Chamaillard et al. 2003a; Girardin et al. 2003b; Girardin et al. 2003a; Inohara et al. 2003). In contrast, the PG-sensing pathway controlled by Nod2 does not recognize this product (Chaput et al. 2006; Nigro et al. 2008).

Here we show that EnhC binds to the *L. pneumophila* Slt and interferes with its function. The primary consequence of EnhC activity is to facilitate intracellular growth of *L. pneumophila* by reducing host cell Nod1 innate immune recognition of bacteria

## Results

### ***L. pneumophila* EnhC directly interacts with soluble lytic murein transglycosylase (Slt)**

There is little information that suggests a function for EnhC, although strains lacking the protein are osmotically unstable (Liu et al. 2008). To identify binding partners of EnhC, a His-tagged derivative of EnhC was purified (Supplemental Fig. S1A), coupled to Affigel-10 beads, and used to isolate proteins from *L. pneumophila* lysates (Experimental Procedures). With beads linked to EnhC, we identified a 66 kDa band not present after elution from control beads (Fig. 1A). The band identified by mass spectrometry was a 606 amino acid protein annotated as soluble lytic murein transglycosylase (Slt; Lpg0663) (Chien et al. 2004) because it shares 29% identity to Slt of *E. coli*. This *L. pneumophila* ortholog of the *E. coli* protein will be referred to as SltL and is predicted to have a periplasmic locale, consistent with previous localization data for EnhC (Liu et al. 2008).

To test whether SltL directly binds EnhC, we incubated purified EnhC with Glutathione-Sepharose beads bound to GST-SltL and the amount of EnhC retained was analyzed by Western blot (Experimental Procedures). The majority of EnhC was pulled down by GST-SltL, whereas only trace amounts of EnhC were left in the supernatant (Fig. 1B). No such binding of EnhC was observed with GST beads.

The *E. coli* Slt enzyme, which we will refer to as SltE, shows optimal cell wall hydrolysis at pH = 4.5 (Holtje et al. 1975). As the activity of the enzyme is measured at pH = 4.5, but the protein likely acts in the periplasm at neutral pH, we wanted to ensure that purified SltL (Supplemental Fig. S1B) bound to EnhC at both acidic and neutral pH, using an enzyme-linked immunosorbent assay (ELISA). Half-maximal binding of EnhC to SltL at pH = 7.4 was obtained at an EnhC concentration of 2 nM (Fig. 1C), while the half-maximal binding at pH = 4.5 was similar (Fig. 1D). EnhC did not bind to bovine serum albumin (BSA)-coated plates under both tested pH conditions (Fig. 1C,1D), indicating that the observed interaction between SltL and EnhC was not dependent on the buffer. We also measured the binding of purified *E. coli* SltE (Supplemental Fig. S1C) to EnhC. Although SltE bound to EnhC at both pH conditions (Fig. 1C, 1D, dashed lines), the half-maximal binding of SltE for EnhC was 10 fold lower than that of SltL for EnhC.

### ***L. pneumophila* SltL catalyzes transglycosylation of *L. pneumophila* peptidoglycan (PG)**

SltE cleaves the  $\beta$ -1,4-glycosidic bond between MurNAc and GlcNAc and generates an intramolecular 1,6-anhydro bond between the C1 and C6 positions in the sugar ring of MurNAc (Fig. 2A). If the short peptide on MurNAc is not cross-linked, then GlcNAc-1,6-anhydro-MurNAc-tetrapeptide (anhydro-disaccharide-tetrapeptide or anhdSTP) is produced, a species of 921 Da (Fig. 2A) (Scheurwater et al. 2008). To determine that *L. pneumophila* SltL is a lytic murein transglycosylase, PG was prepared from a lysate of *L. pneumophila* (Experimental Procedures), incubated with purified SltL in pH 4.5 buffer for 16 hr at 37°C and analyzed by high performance liquid chromatography (HPLC) (Experimental Procedures). Incubation of *L. pneumophila* PG with SltL, yielded a prominent peak that overlapped with the elution peak of pure *E. coli* anhdSTP. No such peak was observed in absence of added SltL (Fig. 2B). MALDI-TOF mass spectrometry (MS) analysis showed that the peak fraction consisted primarily of anhdSTP•Na<sup>+</sup> ( $m/z$  944) and anhdSTP•K<sup>+</sup> ( $m/z$  960) (Fig. 2C). Therefore, SltL has lytic transglycosylation activity against *L. pneumophila* PG.

### ***L. pneumophila* EnhC inhibits the enzymatic activity of *L. pneumophila* SltL**

As EnhC directly binds to SltL, we tested whether EnhC controls the production of anhdSTP by SltL. Purified EnhC was added to the mixture of *Legionella* PG and SltL

(Experimental Procedures) at a 1:1 molar ratio of EnhC :SltL and Slt enzymatic activity was measured at pH = 4.5. The addition of equimolar EnhC to SltL interfered with the production of anhDSTP during a 1 hr reaction, whereas adding the same molar amount of GST had no effect (Fig. 3A, Supplemental Fig. S2). To characterize further the effect of EnhC on the activity of SltL, EnhC or GST was added to SltL-catalyzed reactions and the amount of anhDSTP product was determined over time (Experimental Procedures). The product of each reaction was separated by HPLC and the amount of anhDSTP was plotted as a function of the time of reaction (Fig. 3B). After 30 min. of reaction time, equimolar amounts of SltL and EnhC generated only 30% of the product observed when SltL was incubated in the presence of GST (Fig. 3B).

Although *L. pneumophila* SltL shares 29% identity and 47% similarity with *E. coli* SltE, there is no apparent EnhC ortholog in *E. coli*. To determine whether inhibition by EnhC is specific for SltL, the effect of EnhC on SltE-mediated hydrolysis of *L. pneumophila* PG was tested. The SltL or SltE preparations were incubated with *L. pneumophila* PG for 16 hr and the production of anhDSTP by SltL or SltE was quantified (Fig. 3C). As expected, SltE was active on *L. pneumophila* PG and released anhDSTP from *L. pneumophila* PG. Nevertheless, the generation of anhDSTP by SltL appeared more robust than that by SltE, suggesting a lower activity of SltE on *L. pneumophila* PG. To examine whether EnhC inhibits SltE, *L. pneumophila* PG was incubated with SltE for 1hr with or without EnhC added (Fig. 3D). There was no effect on the production of anhDSTP. On the other hand, adding equimolar amounts of EnhC to SltL still caused about 50% reduction of anhDSTP during a 1hr reaction (Fig. 3D). This result supports the idea that EnhC shows species specificity for inhibition of Slt activity.

### Misregulation of SltL results in enhanced NF- $\kappa$ B activation and depressed growth within macrophages

To determine if the observed lowered intracellular growth was the consequence of a hyperactive SltL protein, we constructed deletions of *sltL* (Supplemental Fig. S3). The  $\Delta$ *sltL* mutant was elongated relative to the wild type strain, grew slowly in broth culture and could not reach post-exponential phase, which is required for optimal intracellular infection. This prevented analysis of intracellular growth, so strains overexpressing SltL were analyzed (Supplemental Fig. S3, WT/*psltL*<sup>+</sup>). Within mouse bone marrow derived macrophages (BMDM), an SltL-overexpressing strain showed growth defects that were strikingly similar to the  $\Delta$ *enhC* mutant, (WT/*psltL*<sup>+</sup>; Fig. 4A). Furthermore, over-expression of SltL in the  $\Delta$ *enhC* mutant ( $\Delta$ *enhC*/*psltL*<sup>+</sup>; Fig. 4A) enhanced the intracellular growth defect of  $\Delta$ *enhC*, indicating that the depression in intracellular growth was proportional to the level of SltL in the cell.

SltL generates the iE-DAP moiety (Fig. 2A), which activates host cell NF- $\kappa$ B response via the Nod1 sensor (Magalhaes et al. ; Chaput et al. 2006; Fritz et al. 2006; Hasegawa et al. 2006; Benko et al. 2008; Nigro et al. 2008). Unregulated SltL should result in excess anhDSTP, consequently triggering a Nod1-dependent NF- $\kappa$ B response (Viala et al. 2004). To test this hypothesis, activation of NF- $\kappa$ B in HEK 293T cells challenged with *L. pneumophila* was quantified by measuring luminescence produced by an NF- $\kappa$ B driven luciferase reporter (Experimental Procedures). *L. pneumophila* overexpressing SltL (WT/*psltL*<sup>+</sup>; Fig. 4B) or lacking EnhC ( $\Delta$ *enhC*, Fig. 4B) caused hyperactivation of NF- $\kappa$ B when compared to controls (WT or WT/pJB908, Fig. 4B). Therefore, overexpression of SltL mimics a strain lacking EnhC in regard to NF- $\kappa$ B activation.

To examine whether hyperactivation of NF- $\kappa$ B was dependent on peptidoglycan sensing by Nod1, siRNA knockdown of Nod1 was performed (Experimental Procedures). Depletion of Nod1 in HEK 293T cells was confirmed by Western blot (Supplemental Figure, Fig. S3,

pSiNod1construct2). As shown in Figure 4C, NF- $\kappa$ B activation elicited by the challenge of WT bacteria was reduced by 50% in cells depleted of Nod1 (SiNod1) compared to cells having a control siRNA knockdown (SiEGFP). Therefore, a significant portion of NF- $\kappa$ B activation in response to *L. pneumophila* was triggered *via* Nod1. Strikingly, hyperactivation of NF- $\kappa$ B in response to either the  $\Delta$ enhC strain or the strain overexpressing SltL (WT/*psltL*<sup>+</sup>) was abolished in cells knocked down with SiNod1 (Fig. 4C). Hyperactivation by the  $\Delta$ enhC strain could also be reversed by introducing *enhC* on a plasmid ( $\Delta$ enhC/*penhC*<sup>+</sup>; Fig. 4B and 4C). To determine if a similar increase in NF- $\kappa$ B activation could be seen in bone marrow macrophages, activation was measured using a different assay (Losick and Isberg 2006), quantitating the fraction of infected C57BL/6 *myd88*<sup>-/-</sup> macrophages that had observable NF- $\kappa$ B p65 nuclear translocation. Bacterial strains used here were  $\Delta$ flaA (flagellin deficient) to prevent the Naip5/Birc1e signaling that occurs in the C57BL/6 mouse background. This assay did not detect an increase in p65 translocation when macrophages from *myd88*<sup>-/-</sup> mice were used to limit the TLR signaling contribution (Fig. 4D). This is either because these two readouts show different levels of sensitivity to changes in NF- $\kappa$ B activation, MyD88 signals that collaborate with Nod1 in HEK 293T cells could not be detected in these macrophages, or else the Nod1-dependent response observed in the HEK 293T is independent of NF- $\kappa$ B activation. The latter model will be treated in the Discussion.

### **Inhibition of SltL by EnhC is required to suppress Nod1-dependent NF- $\kappa$ B activation induced by *L. pneumophila***

To further demonstrate that lack of inhibition of SltL by EnhC is responsible for the phenotype of the  $\Delta$ enhC mutant, we tested whether lowering Slt activity in *L. pneumophila* could bypass the EnhC requirement. As *L. pneumophila* $\Delta$ sltL was defective for growth in broth culture, deleting *sltL* in a strain lacking EnhC was not feasible. Instead, *sltL* was substituted with *E. coli* *sltE* gene on the *L. pneumophila* chromosome to generate a new strain predicted to have lowered Slt activity (MLL1001;  $\Delta$ sltL::*sltE*<sup>+</sup>) (Fig. 5A). The SltE protein had lowered activity on *L. pneumophila* PG (Fig. 3C) and transcription of *sltE* in *L. pneumophila* was about 20% that of *sltL* as monitored by qRT-PCR (Experimental Procedures; Supplemental Fig. S4). When the  $\Delta$ sltL::*sltE*<sup>+</sup> strain was used to challenge mouse BMDMs, it had the same intracellular growth rate as WT *L. pneumophila*, indicating that there was sufficient Slt activity to support growth in a number of conditions (Fig. 5B). This predicts that altering Slt activity in *L. pneumophila* should make EnhC dispensable for intracellular growth and normal level of Nod1-dependent NF- $\kappa$ B activation. To test this hypothesis, the  $\Delta$ sltL::*sltE*<sup>+</sup> replacement was moved into a  $\Delta$ enhC background (Supplemental Fig. S4). Nod1-dependent NF- $\kappa$ B activation in response to the  $\Delta$ enhC  $\Delta$ sltL::*sltE*<sup>+</sup> strain was similar to that observed for either WT bacteria or the  $\Delta$ sltL::*sltE*<sup>+</sup> strain (Fig. 5C), indicating that hyperactivation resulting from loss of EnhC was dependent on having a wild type *sltL* allele.

### **Nod1 and products of soluble lytic transglycosylase are responsible for the intracellular growth defect of the $\Delta$ enhC mutant**

To evaluate the importance of EnhC and the reduced Nod1 sensing resulting from the presence of EnhC, we monitored the intracellular growth of a variety of *Legionella* strains. Intracellular growth of the  $\Delta$ enhC mutant is known to be restricted at a time point roughly corresponding to 24-48 hr post-infection (hpi) (Liu et al. 2008). To test whether the restriction of  $\Delta$ enhC strain was due to an inability to regulate the activity of SltL, intracellular growth in BMDMs of both the  $\Delta$ enhC and the  $\Delta$ enhC $\Delta$ sltL::*sltE*<sup>+</sup> strains was monitored (Fig. 6A). The  $\Delta$ enhC mutant replicated at the same rate as WT in the first round of intracellular growth (24 hpi) and showed a defect in growth at 48 hpi, consistent with previous observations (Liu et al. 2008). In contrast, the  $\Delta$ enhC strain harboring the



$\Delta sltL::sltE^+$  replacement grew as well as WT at 48 hpi (Fig. 6A). This result is consistent with the dependence of the intracellular growth defect of  $\Delta enhC$  on the *slt* allele.

Results from Figs 5C and 6A indicated that reduced production of anhDSTP caused by a low level of Slt was responsible for rescue of the  $\Delta enhC$  mutant. To examine this further, we tested whether overexpression of *sltE* had a similar phenotype to overproduction of SltL. Plasmid-borne *sltE* was introduced into the  $\Delta enhC \Delta sltL::sltE^+$  replacement strain, and overexpression of *sltE* was confirmed by qRT-PCR (Supplemental Fig. S4). Overexpression of *sltE* reduced intracellular growth at 48 hpi (Fig. 6B;  $\Delta enhC \Delta sltL::sltE^+/psltE^+$ ). The presence of an intact *enhC* gene did not alter these results, as the  $EnhC^+$  replacement strain overproducing SltE also showed a significantly reduced intracellular growth at 48 hpi (Fig. 6C;  $\Delta sltL::sltE^+/psltE^+$ ). These results are consistent with unregulated production of anhDSTP being responsible for the intracellular growth defect of  $\Delta enhC$ . Furthermore, it is unlikely that the mutant phenotype of a  $\Delta enhC$  strain is due to SltL having a unique activity not catalyzed by SltE.

As Slt activity appears tightly linked to the phenotype of a  $\Delta enhC$  strain, we tested whether EnhC promotes intracellular growth of *L. pneumophila* by limiting Nod1 sensing of anhDSTP. Therefore, the intracellular growth of the mutant lacking EnhC was examined in BMDMs from C57BL/6 mice having the  $Nod1^{-/-}$ ,  $Nod2^{-/-}$  and  $RIP2^{-/-}$  (defective for both Nod1 and Nod2 signaling) genotypes. All bacterial strains used in this assay were  $\Delta flaA$  (flagellin deficient) to prevent the Naip5/Birc1e signaling that occurs in the C57BL/6 mouse background (Supplemental Fig. S5). In macrophages prepared from either RIP2 or Nod1 knockout mice, defective intracellular growth due to the  $\Delta enhC$  mutation was no longer apparent (Fig. 7; for  $nod1^{-/-}$ ,  $P = 0.61$ ; for  $rip2^{-/-}$ ,  $P = 0.64$  by unpaired Student's *t*-test). In contrast, the growth defect of  $\Delta enhC$  was maintained in the Nod2 knockout macrophages, which, unlike  $Nod1^{-/-}$  and  $RIP2^{-/-}$  macrophages, still retain the ability to recognize anhDSTP ( $P = 0.002$ ). These observations support the model that EnhC promotes intracellular growth of *L. pneumophila* by interfering with Nod1 signaling.

## Discussion

In this study we showed that EnhC modulates the activity of SltL transglycosylase, generating the identical anhydro-disaccharide-tetrapeptide (anhDSTP) produced by *E. coli* soluble lytic transglycosylase. EnhC binding to *L. pneumophila* SltL interferes with PG degradation, indicating that mutants lacking EnhC likely increase the amount of anhDSTP available to host cells. Negative regulation of SltL by EnhC provides an explanation for the previous observation that the absence of EnhC results in enhanced sensitivity to a variety of stress-inducing reagents (Liu et al. 2008). Presumably, unregulated SltL results in a loss of PG integrity.

The negative regulation of SltL activity by EnhC allows growth phase control of peptidoglycan degradation. The levels of SltL protein are similar at all phases of *L. pneumophila* growth (Supplemental Fig. S5), whereas EnhC is highly expressed in post-exponential phase (Liu et al. 2008). During growth and division of *L. pneumophila*, expression of SltL in the absence of EnhC may allow modulation of PG structure, facilitating septation (Heidrich et al. 2002) and insertion of protein complexes in the cell envelope (Koraimann 2003). When growth slows and bacteria enter post-exponential phase, PG turnover becomes less important, and cell envelope integrity becomes paramount. Although the transglycosylase could be regulated by proteolytic turnover, the presence of an inhibitory protein offers a clear advantage. Proteolysis could remove the entire pool of SltL from the periplasm, reducing enzyme concentration below the basal level necessary for

maintaining PG homeostasis. In contrast, modulation by a protein inhibitor allows basal levels of enzyme activity controlled by the concentration of EnhC.

Association of soluble lytic transglycosylase with periplasmic proteins has been demonstrated previously. Slt from *Pseudomonas aeruginosa* has been found to associate with PG synthase-PBP2 (Legaree and Clarke 2008) and Slt from *Brucella suis* was found to interact with protein complexes of the Type IV secretion system (Hoppner et al. 2005). Such physical associations could, in the first case, allow coordination of PG degradation and synthesis. In the second example, the association of Slt with the Type IV secretion system may facilitate the assembly of this complex, allowing it to extend through PG layers by generating space for its insertion (Koraimann 2003).

The data from the HEK 293T cell reporter assay are consistent with the Nod1 effects associated with the *enhC*<sup>-</sup> mutant being mediated *via* an NF- $\kappa$ B-dependent pathway. In contrast, the link between NF- $\kappa$ B activation and Nod1 restriction in bone marrow macrophages is not as clear. Although Nod1 was required to selectively restrict the *enhC*<sup>-</sup> mutant in bone marrow macrophages, we did not observe enhanced kinetics of p65 translocation in response to the mutant bacterium (Fig. 4D). This is consistent with Nod1-restriction acting *via* an alternate pathway in macrophages. It is now apparent that restriction of bacterial growth resulting from Nod1 activation can occur independently of NF- $\kappa$ B activation, as *Shigella flexneri* infection stimulates a Nod1-associated NF- $\kappa$ B-independent antimicrobial response that recruits a subset of cellular autophagy components (Travassos et al. 2010). A similar strategy for restriction of *L. pneumophila* growth may be occurring in macrophages, so that Nod1 activation results in different responses in different cell types.

The Nod1 response is stimulated by a variety of microorganisms (Girardin et al. 2001; Kim et al. 2004; Viala et al. 2004; Travassos et al. 2005; Nigro et al. 2008; Archer et al. 2010), arguing that EnhC impinges on an important arm of innate immunity. Pathogenic bacteria manage to escape from Nod sensing using a variety of strategies, including modifying PG components, changing the composition of PG and efficiently recycling muramylpeptides back to the bacterial cytosol (Chamaillard et al. 2003b; Psylinakis et al. 2005; Chaput et al. 2006; Boneca et al. 2007; Davis et al. 2008; Nigro et al. 2008). Our data present another strategy, which is to inhibit the major enzyme generating anhydro-muramylpeptides.

Nod1 signaling is associated with immune surveillance in multicellular eukaryotes, so the selective pressures that resulted in the retention of EnhC function are not obvious. It is thought that the pressures that sculpted the *L. pneumophila* genome selected for a bacterium able to grow in a wide variety of amoebal species. Consistent with this model, there is little evidence for *L. pneumophila* directly interfering with host innate immune sensing pathways (Shin et al. 2008), and it seems unlikely that the mammalian host immune system exerted selective pressure. Rather, the enhanced stress resistance conferred by EnhC on post-exponential phase bacteria is probably the primary selective advantage for retention of this gene. Alternatively, EnhC may be important for survival in the presence of killing strategies used by an amoebal host that is found in the environment but not interrogated in this work.

For bacteria with access to host cell cytosol, such as *Shigella flexneri*, muramylpeptides resulting from PG turnover can be shed directly into cytosol and detected by Nod1 (Nigro et al. 2008). For bacteria residing in vacuoles, such as *L. pneumophila*, it is unclear how hydrophilic muramylpeptides can cross the vacuolar membrane and be sensed by Nod1. Presentation of *Helicobacter pylori* muramylpeptides to cytosolic Nod1 is dependent on the CagPAI-encoded Type IV secretion system (Viala et al. 2004), so it is possible that muramylpeptides from *L. pneumophila* could be presented through the Icm/Dot secretion system. Strains defective for Icm/Dot show very low activation of NF- $\kappa$ B in HEK 293T

cells (Losick and Isberg 2006), indicating that muramylpeptide stimulation of host cells requires a functional Type IV secretion system. In further support of this model, both NF- $\kappa$ B activation and activation of multiple MAP kinases by the Nod signaling pathway require the Icm/Dot system (Shin et al. 2008). It seems likely that release *via* Icm/Dot might act as the mechanism for PG presentation.

It is not clear how Nod1 recognition leads to restriction of *L. pneumophila*. Nod1 recognition can trigger a variety of host immune responses, including macrophage priming and the production of various cytokines, chemokines and antimicrobial peptides, as well as autophagic response described above (Boneca 2005; Chaput and Boneca 2007; Travassos et al. 2010). Previous work has shown that Nod1 activity plays a role in interfering with bacterial survival in the presence of a variety of cell types, including fibroblasts (Travassos et al. 2005) and bone marrow-derived dendritic cells (Le Bourhis et al. 2009). In addition, Nod1 controls the expression of a subset of  $\beta$ -defensin anti-microbial peptides (Grubman et al. 2010). Strategies such as these, combined with the inherent increased instability of the bacterial cell wall, could contribute to the reduced yield of the *enhC*<sup>-</sup> mutants when exposed to macrophages.

In summary, our work uncovers a mechanism for regulating the activity of soluble lytic transglycosylase. This mechanism allows high viability of *L. pneumophila* in the presence of increased stress and allows the integrity of the bacterial envelope to be maintained during post-exponential phase in which a large number of bacterial products are poised to be deposited in host cells.

## Experimental Procedures

### Bacterial strains, plasmids, reagents and cell culture

All bacterial strains and plasmids used in this work are listed in Table 1. All PCR primers are listed in Supplementary Table S1. Charcoal Yeast Extract agar (CYE) and ACES buffered Yeast Extract (AYE) broth were used to cultivate *Legionella pneumophila* in culture as described (Feeley et al. 1979; Berger and Isberg 1993). Thymidine was added at a concentration of 100  $\mu$ g/ml when needed.

Plasmids were constructed as described in Supplemental Data. pHis-SltE (pMLD204) was a kind gift of Dr. Dominique Mengin-Lecreux (University Paris-Sud, Orsay, France).

Mouse bone marrow derived macrophages (BMDM) were prepared from the femurs of female A/J mice (Jackson Laboratories) or mouse strains-RIP2<sup>-/-</sup>, Nod-1<sup>-/-</sup>, and Nod-2<sup>-/-</sup> (generous gifts of Dr. Koichi S. Kobayashi, Dana Farber Cancer Center, Boston, MA) (Dietrich et al. 1995) and cultivated in RPMI 1640 (Invitrogen-Gibco) with 10% heat-inactivated fetal bovine serum (FBS) (Gibco). HEK 293T cells (ATCC CRL-11268) were passaged in high glucose DMEM media containing 4.5g/L D-Glucose (Cat. 11995, Invitrogen-Gibco) supplemented with 10% heat-inactivated Hyclone FBS (Thermo Scientific).

### Affinity Chromatography from *Legionella* lysates

200 ml of post-exponential phase ( $A_{600} = 3.7\sim 3.9$ ) motile *Legionella pneumophila* culture was pelleted at  $9,000 \times g$  for 15 min at 4 °C, then resuspended in 10 ml ice-cold lysis buffer (PBS, 1 mM  $\beta$ -mercaptoethanol [ $\beta$ -ME], protease inhibitor cocktail [Roche]) and lysed by French press at 1000 psi (Thermo Electron) and cleared by 2x centrifugation at  $10,000 \times g$ . Lysate from approximately  $7.4 \times 10^{10}$  bacteria, was incubated with 75  $\mu$ l Affigel-10 beads linked to approximately 90  $\mu$ g EnhC for 12 hr at 4°C. Beads were washed 4 or 5 times with ice-cold lysis buffer, resuspended in 12  $\mu$ l SDS sample buffer, and boiled for 5 min and



analyzed by 10 % SDS-PAGE and silver staining (Invitrogen). Proteins were isolated from gels and analyzed by high-performance liquid chromatography/mass spectrometry (HPLC/MS) (Tufts University proteomics core facility).

### Recombinant protein purification, anti-SltL antibody production and assay for binding of purified proteins

Details of protein purification are found in Supplemental Data. Purified SltL was injected into rabbits to raise anti-SltL serum (Pocono Rabbit Farm and Laboratory Inc.). Anti-SltL antibody recognized a single protein band with predicted size from LP02 (WT) extract using dilution of 1: 5000 when  $5 \times 10^7$  bacteria were loaded, but did not recognize any protein from *ΔsltL* extracts. To analyze binding to SltL, purified EnhC was incubated with GST-SltL bound to GS beads for 12 hr at 4°C. Beads were washed 4 times with PBS, then resuspended and boiled in SDS sample buffer before analysis by Western blot with polyclonal antibody specific for EnhC (1: 10,000 dilution) (Liu et al. 2008).

### Quantitative measurement of Slt and EnhC interaction

Interactions between purified EnhC and either purified SltL or purified SltE were measured using ELISA. Each well of ELISA plates (Linbro) was coated with 100 μl of 100 nM SltL or SltE or BSA in PBS at 4°C for over night. Wells were washed three times with PBS, then were blocked with 3% BSA in PBS at 4°C for over night. Wells were washed once with PBS before probing with sequential 3-fold dilutions of EnhC starting at a concentration of 1500 nM in either PBS buffer (pH = 7.4) or PBS supplemented with 0.01 M sodium acetate (pH = 4.5) and 0.05 M MgCl<sub>2</sub> for 2 hr at room temperature. Wells were washed six times with PBS. EnhC bound to wells was detected by probing wells with rabbit anti-EnhC polyclonal antibody (Liu *et al.*, 2008) for 90 min at room temperature. Wells were subjected to 6 washes with PBS before probing with goat anti-rabbit IgG conjugated to alkaline phosphatase (Zymed-Invitrogen) for 90 min at room temperature. Wells were washed 6 times with PBS before phosphatase activity was detected with 3 mM PNPP (Sigma 104 phosphatase substrate, Sigma) in 0.05 M Na<sub>2</sub>CO<sub>3</sub> (pH = 8.5) and 0.05 mM MgCl<sub>2</sub>. The reactions were stopped with 0.2 M NaOH after about 25 min.

### Preparation of peptidoglycan (PG) from *Legionella pneumophila*

Peptidoglycan was prepared as described (Uehara and Park 2003). Further details on its isolation can be found in Supplemental Materials.

### Digestion of *L. pneumophila* peptidoglycan (PG) by soluble lytic transglycosylase (Slt) and high performance liquid chromatography (HPLC) analysis

50 μg of *L. pneumophila* PG was incubated with about 3 μg of purified *L. pneumophila* or *E. coli* Slt in 100 μl of reaction buffer (10 mM NaAc [pH=4.5], 50 mM MgCl<sub>2</sub>) at 37°C. The undigested PG was cleared by ultracentrifugation at 130,000 × *g* for 55 min and the supernatant was separated by Sunfire™ C18 reverse-phase column (4.6 × 150 mm; particle size, 5 μm; Waters Co., Milford, MA) using a Waters 1525 binary HPLC pump. The column was equilibrated by solvent A at a flow rate of 0.5 ml/min for 15 min. Then samples were injected and separated at a flow rate of 0.5 ml/min with a linear gradient of 0 to 10% solvent B over a period of 5 min, followed by a linear gradient of 10 to 50% solvent B over a period of 25 min. Solvent A: 25mM formic acid (HCOOH), 12.5mM ammonium hydroxide (NH<sub>4</sub>OH), pH = 3.75. Solvent B: 25mM HCOOH, 12.5mM NH<sub>4</sub>OH and 80% Methanol (MeOH). For mass spectrometry (MS), 150 μg of PG instead of 50 μg was digested for 16 hr and separated by HPLC. The main fraction was collected, lyophilized, and identified by MS with a Voyager DE Pro matrix-assisted laser desorption ionization—time-of-flight (MALDI-TOF) mass spectrometer (Applied Biosystems) at Tufts University Core Facility.

## NF- $\kappa$ B activation assays

For NF- $\kappa$ B activation, assays in HEK293T cells were performed as described, challenging cells with bacteria for 8 hours at MOI = 0.05 or = 1 (Losick et al. 2010). For NF- $\kappa$ B assays in siRNA-treated HEK293T cells, cells were transfected with 100ng endotoxin-free psiRNA (ie SiEGFP or SiNod1) per well using 0.25 $\mu$ l Lipofectamine 2000 in total 50 $\mu$ l OPTI-MEM. After 20 hrs, cells were observed under fluorescence microscope to ensure there was efficient transfection by determining that greater than 75% of the cells showed GFP fluorescence. Media were changed and cells were transfected with endotoxin-free pNF- $\kappa$ B-luciferase reporter plasmid (Losick et al. 2010). 18 hrs later, cells were infected with bacteria at M.O.I. = 1. *L. pneumophila* uptake into HEK293T cells was monitored in all NF- $\kappa$ B assays to ensure that the NF- $\kappa$ B activation measurements were not affected by bacterial load. For p65 translocation assays, bone marrow macrophages were challenged with bacteria at M.O.I. = 1.0 and p65 nuclear translocation was determined by indirect immunofluorescence microscopy, probing fixed cells with anti-p65 (Losick and Isberg 2006). 100 cells per coverslip were counted visually.

## Nod1 psiRNA constructs and assay for testing the efficiency of knockdown constructs

Construction of siRNA plasmids can be found in Supplemental Data. To test the knockdown efficiency of psiNod1, HEK293T cells were cotransfected with 10ng pmyc-Nod1 and 200ng of psiEGFP or psiNod1. 48 hrs later, cells were lysed and analyzed by Western blot with anti-myc to determine steady state protein level of myc-Nod1.

## Quantitative Real-time PCR (QRT-PCR) assay of *slt* transcripts in *L. pneumophila*

Primers for QRT-PCR are listed in Supplemental Table 2. RNA and genomic DNA (gDNA) from *L. pneumophila* were extracted using the RNeasy and DNeasy miniprep kits (Qiagen). QRT-PCR reactions were set up in 96 well polypropylene plates (Stratagene) using real-time PCR machine Mx3005 model (Stratagene). DNA-free RNA samples in the absence of reverse transcriptase incubation were also included in QRT-PCR to ensure that there was no gDNA contamination in cDNA samples. All QRT-PCR reactions were normalized with 16s ribosome RNA as the internal control. Means  $\pm$  s.d. were generated from triplicate QRT-PCR reactions.

## Supplementary Material

Refer to Web version on PubMed Central for supplementary material.

## Acknowledgments

We want to thank Dr. Koichi S. Kobayashi for providing bone marrows of RIP2<sup>-/-</sup>, Nod1<sup>-/-</sup> and Nod2<sup>-/-</sup> mice, Dr. Dominique Mengin-Lecreulx for providing the *E. coli* SltE expression plasmid pMLD204 and Dr. Waldemar Vollmer for the *E. coli*  $\Delta$ sltE strain MUF16, respectively, as well as Dr. Tao Ren for providing the *L. pneumophila*  $\Delta$ flaA strain. We would also like to thank Drs. Edward Geisinger, Dervla Isaac, Eva Haenssler, Kerri Sheahan, Elizabeth Creasey, Sina Mohammadi and Greg Crimmins for comments on the text. RI is an Investigator of the Howard Hughes Medical Institute (HHMI). This work was supported by HHMI.

## REFERENCES

- Amer A, Franchi L, Kanneganti TD, Body-Malapel M, Ozoren N, et al. Regulation of *Legionella* phagosome maturation and infection through flagellin and host Ipaf. *J Biol Chem*. 2006; 281(46): 35217–35223. [PubMed: 16984919]
- Archer KA, Roy CR. MyD88-dependent responses involving toll-like receptor 2 are important for protection and clearance of *Legionella pneumophila* in a mouse model of Legionnaires' disease. *Infect Immun*. 2006; 74:3325–3333. [PubMed: 16714560]

- Archer KA, Alexopoulou L, Flavell RA, Roy CR. Multiple MyD88-dependent responses contribute to pulmonary clearance of *Legionella pneumophila*. *Cell Microbiol.* 2009; 11:21–36. [PubMed: 18782351]
- Archer KA, Ader F, Kobayashi KS, Flavell RA, Roy CR. Cooperation between multiple microbial pattern recognition systems is important for host protection against the intracellular pathogen *Legionella pneumophila*. *Infect Immun.* 2010; 78:2477–2487. [PubMed: 20351139]
- Bartfeld S, Engels C, Bauer B, Aurass P, Flieger A, et al. Temporal resolution of two-tracked NF- $\kappa$ B activation by *Legionella pneumophila*. *Cell Microbiol.* 2009; 11(11):1638–1651. [PubMed: 19573161]
- Benko S, Philpott DJ, Girardin SE. The microbial and danger signals that activate Nod-like receptors. *Cytokine.* 2008; 43:368–373. [PubMed: 18715799]
- Berger KH, Isberg RR. Two distinct defects in intracellular growth complemented by a single genetic locus in *Legionella pneumophila*. *Mol Microbiol.* 1993; 7:7–19. [PubMed: 8382332]
- Berger KH, Merriam JJ, Isberg RR. Altered intracellular targeting properties associated with mutations in the *Legionella pneumophila* dotA gene. *Mol Microbiol.* 1994; 14:809–822. [PubMed: 7891566]
- Boneca IG. The role of peptidoglycan in pathogenesis. *Curr Opin Microbiol.* 2005; 8:46–53. [PubMed: 15694856]
- Boneca IG, Dussurget O, Cabanes D, Nahori MA, Sousa S, et al. A critical role for peptidoglycan N-deacetylation in *Listeria* evasion from the host innate immune system. *Proc Natl Acad Sci U S A.* 2007; 104:997–1002. [PubMed: 17215377]
- Burstein D, Zusman T, Degtyar E, Viner R, Segal G, et al. Genome-scale identification of *Legionella pneumophila* effectors using a machine learning approach. *PLoS Pathog.* 2009; 5:e1000508. [PubMed: 19593377]
- Chamaillard M, Girardin SE, Viala J, Philpott DJ. Nods, Nalps and Naip: intracellular regulators of bacterial-induced inflammation. *Cell Microbiol.* 2003a; 5:581–592. [PubMed: 12925128]
- Chamaillard M, Hashimoto M, Horie Y, Masumoto J, Qiu S, et al. An essential role for NOD1 in host recognition of bacterial peptidoglycan containing diaminopimelic acid. *Nat Immunol.* 2003b; 4:702–707. [PubMed: 12796777]
- Chaput C, Boneca IG. Peptidoglycan detection by mammals and flies. *Microbes Infect.* 2007; 9:637–647. [PubMed: 17383922]
- Chaput C, Ecobichon C, Cayet N, Girardin SE, Werts C, et al. Role of AmiA in the morphological transition of *Helicobacter pylori* and in immune escape. *PLoS Pathog.* 2006; 2:e97. [PubMed: 17002496]
- Chien M, Morozova I, Shi S, Sheng H, Chen J, et al. The genomic sequence of the accidental pathogen *Legionella pneumophila*. *Science.* 2004; 305:1966–1968. [PubMed: 15448271]
- Davis KM, Akinbi HT, Standish AJ, Weiser JN. Resistance to mucosal lysozyme compensates for the fitness deficit of peptidoglycan modifications by *Streptococcus pneumoniae*. *PLoS Pathog.* 2008; 4:e1000241. [PubMed: 19079576]
- de Felipe KS, Pampou S, Jovanovic OS, Pericone CD, Ye SF, et al. Evidence for acquisition of *Legionella* type IV secretion substrates via interdomain horizontal gene transfer. *J Bacteriol.* 2005; 187:7716–7726. [PubMed: 16267296]
- Dietrich WF, Damron DM, Isberg RR, Lander ES, Swanson MS. Lgn1, a gene that determines susceptibility to *Legionella pneumophila*, maps to mouse chromosome 13. *Genomics.* 1995; 26:443–450. [PubMed: 7607666]
- Feeley JC, Gibson RJ, Gorman GW, Langford NC, Rasheed JK, et al. Charcoal-yeast extract agar: primary isolation medium for *Legionella pneumophila*. *J Clin Microbiol.* 1979; 10:437–441. [PubMed: 393713]
- Fraser DW, Tsai TR, Orenstein W, Parkin WE, Beecham HJ, et al. Legionnaires' disease: description of an epidemic of pneumonia. *N Engl J Med.* 1977; 297:1189–1197. [PubMed: 335244]
- Fritz JH, Ferrero RL, Philpott DJ, Girardin SE. Nod-like proteins in immunity, inflammation and disease. *Nat Immunol.* 2006; 7:1250–1257. [PubMed: 17110941]
- Girardin SE, Travassos LH, Herve M, Blanot D, Boneca IG, et al. Peptidoglycan molecular requirements allowing detection by Nod1 and Nod2. *J Biol Chem.* 2003a; 278:41702–41708. [PubMed: 12871942]

- Girardin SE, Tournebize R, Mavris M, Page AL, Li X, et al. CARD4/Nod1 mediates NF- $\kappa$ B and JNK activation by invasive *Shigella flexneri*. *EMBO Rep.* 2001; 2:736–742. [PubMed: 11463746]
- Girardin SE, Boneca IG, Carneiro LA, Antignac A, Jehanno M, et al. Nod1 detects a unique muropeptide from gram-negative bacterial peptidoglycan. *Science.* 2003b; 300:1584–1587. [PubMed: 12791997]
- Grubman A, Kaparakis M, Viala J, Allison C, Badea L, et al. The innate immune molecule, NOD1, regulates direct killing of *Helicobacter pylori* by antimicrobial peptides. *Cell Microbiol.* 12:626–639. [PubMed: 20039881]
- Hasegawa M, Yang K, Hashimoto M, Park JH, Kim YG, et al. Differential release and distribution of Nod1 and Nod2 immunostimulatory molecules among bacterial species and environments. *J Biol Chem.* 2006; 281:29054–29063. [PubMed: 16870615]
- Hawn TR, Smith KD, Aderem A, Skerrett SJ. Myeloid differentiation primary response gene (88)- and toll-like receptor 2-deficient mice are susceptible to infection with aerosolized *Legionella pneumophila*. *J Infect Dis.* 2006; 193:1693–1702. [PubMed: 16703513]
- Heidrich C, Ursinus A, Berger J, Schwarz H, Holtje JV. Effects of multiple deletions of murein hydrolases on viability, septum cleavage, and sensitivity to large toxic molecules in *Escherichia coli*. *J Bacteriol.* 2002; 184:6093–6099. [PubMed: 12399477]
- Holtje JV. Lytic transglycosylases. *EXS.* 1996; 75:425–429. [PubMed: 8765311]
- Holtje JV, Mirelman D, Sharon N, Schwarz U. Novel type of murein transglycosylase in *Escherichia coli*. *J Bacteriol.* 1975; 124:1067–1076. [PubMed: 357]
- Hoppner C, Carle A, Sivanesan D, Hoepfner S, Baron C. The putative lytic transglycosylase VirB1 from *Brucella suis* interacts with the type IV secretion system core components VirB8, VirB9 and VirB11. *Microbiology.* 2005; 151:3469–3482. [PubMed: 16272371]
- Horwitz MA. Formation of a novel phagosome by the Legionnaires' disease bacterium (*Legionella pneumophila*) in human monocytes. *J Exp Med.* 1983; 158:1319–1331. [PubMed: 6619736]
- Huang L, Boyd D, Amyot WM, Hempstead AD, Luo ZQ, et al. The E-Block motif is associated with *Legionella pneumophila* translocated substrates. *Cell Microbiol.* 2010; 13:227–245. [PubMed: 20880356]
- Inohara N, Ogura Y, Fontalba A, Gutierrez O, Pons F, et al. Host recognition of bacterial muramyl dipeptide mediated through NOD2. Implications for Crohn's disease. *J Biol Chem.* 2003; 278:5509–5512. [PubMed: 12514169]
- Ishii KJ, Koyama S, Nakagawa A, Coban C, Akira S. Host innate immune receptors and beyond: making sense of microbial infections. *Cell Host Microbe.* 2008; 3:352–363. [PubMed: 18541212]
- Kagan JC, Roy CR. *Legionella* phagosomes intercept vesicular traffic from endoplasmic reticulum exit sites. *Nat Cell Biol.* 2002; 4:945–954. [PubMed: 12447391]
- Kim JG, Lee SJ, Kagnoff MF. Nod1 is an essential signal transducer in intestinal epithelial cells infected with bacteria that avoid recognition by toll-like receptors. *Infect Immun.* 2004; 72:1487–1495. [PubMed: 14977954]
- Koraimann G. Lytic transglycosylases in macromolecular transport systems of Gram-negative bacteria. *Cell Mol Life Sci.* 2003; 60:2371–2388. [PubMed: 14625683]
- Laguna RK, Creasey EA, Li Z, Valtz N, Isberg RR. A *Legionella pneumophila*-translocated substrate that is required for growth within macrophages and protection from host cell death. *Proc Natl Acad Sci U S A.* 2006; 103:18745–18750. [PubMed: 17124169]
- Le Bourhis L, Magalhaes JG, Selvanantham T, Travassos LH, Geddes K, et al. Role of Nod1 in mucosal dendritic cells during *Salmonella* pathogenicity island 1-independent *Salmonella enterica* serovar Typhimurium infection. *Infect Immun.* 2009; 77:4480–4486. [PubMed: 19620349]
- Legaree BA, Clarke AJ. Interaction of penicillin-binding protein 2 with soluble lytic transglycosylase B1 in *Pseudomonas aeruginosa*. *J Bacteriol.* 2008; 190:6922–6926. [PubMed: 18708507]
- Lightfield KL, Persson J, Brubaker SW, Witte CE, von Moltke J, et al. Critical function for Naip5 in inflammasome activation by a conserved carboxy-terminal domain of flagellin. *Nat Immunol.* 2008; 9:1171–1178. [PubMed: 18724372]
- Liu M, Conover GM, Isberg RR. *Legionella pneumophila* EnhC is required for efficient replication in tumor necrosis factor alpha-stimulated macrophages. *Cell Microbiol.* 2008

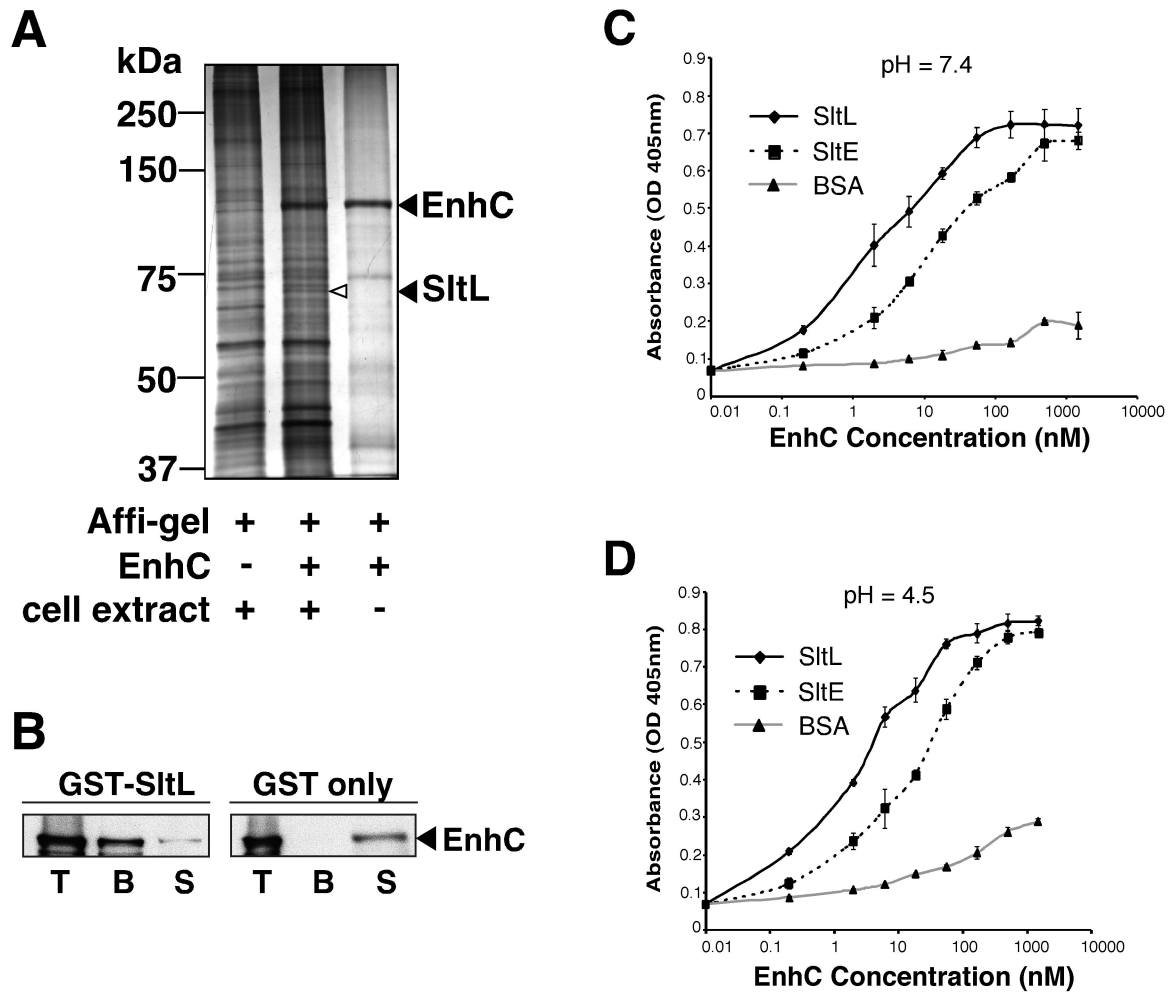
- Losick VP, Isberg RR. NF- $\kappa$ B translocation prevents host cell death after low-dose challenge by *Legionella pneumophila*. *J Exp Med*. 2006; 203:2177–2189. [PubMed: 16940169]
- Losick VP, Haenssler E, Moy MY, Isberg RR. LnaB: a *Legionella pneumophila* activator of NF- $\kappa$ B. *Cell Microbiol*. 2010; 12:1083–1097. [PubMed: 20148897]
- Luo ZQ, Isberg RR. Multiple substrates of the *Legionella pneumophila* Dot/Icm system identified by interbacterial protein transfer. *Proc Natl Acad Sci U S A*. 2004; 101:841–846. [PubMed: 14715899]
- Machner MP, Isberg RR. A bifunctional bacterial protein links GDI displacement to Rab1 activation. *Science*. 2007; 318:974–977. [PubMed: 17947549]
- Magalhaes JG, Sorbara MT, Girardin SE, Philpott DJ. What is new with Nods? *Curr Opin Immunol*. 23:29–34. [PubMed: 21190821]
- McDade JE, Shepard CC, Fraser DW, Tsai TR, Redus MA, et al. Legionnaires' disease: isolation of a bacterium and demonstration of its role in other respiratory disease. *N Engl J Med*. 1977; 297:1197–1203. [PubMed: 335245]
- Molofsky AB, Byrne BG, Whitfield NN, Madigan CA, Fuse ET, et al. Cytosolic recognition of flagellin by mouse macrophages restricts *Legionella pneumophila* infection. *J Exp Med*. 2006; 203:1093–1104. [PubMed: 16606669]
- Nigro G, Fazio LL, Martino MC, Rossi G, Tattoli I, et al. Muramylpeptide shedding modulates cell sensing of *Shigella flexneri*. *Cell Microbiol*. 2008; 10:682–695. [PubMed: 18042252]
- Park JT, Uehara T. How bacteria consume their own exoskeletons (turnover and recycling of cell wall peptidoglycan). *Microbiol Mol Biol Rev*. 2008; 72:211–227. [PubMed: 18535144]
- Psylinakis E, Boneca IG, Mavromatis K, Deli A, Hayhurst E, et al. Peptidoglycan N-acetylglucosamine deacetylases from *Bacillus cereus*, highly conserved proteins in *Bacillus anthracis*. *J Biol Chem*. 2005; 280:30856–30863. [PubMed: 15961396]
- Rankin S, Li Z, Isberg RR. Macrophage-induced genes of *Legionella pneumophila*: protection from reactive intermediates and solute imbalance during intracellular growth. *Infect Immun*. 2002; 70:3637–3648. [PubMed: 12065505]
- Ren T, Zamboni DS, Roy CR, Dietrich WF, Vance RE. Flagellin-deficient *Legionella* mutants evade caspase-1- and Naip5-mediated macrophage immunity. *PLoS Pathog*. 2006; 2:e18. [PubMed: 16552444]
- Rowbotham TJ. Preliminary report on the pathogenicity of *Legionella pneumophila* for freshwater and soil amoebae. *J Clin Pathol*. 1980; 33:1179–1183. [PubMed: 7451664]
- Roy CR, Mocarski ES. Pathogen subversion of cell-intrinsic innate immunity. *Nat Immunol*. 2007; 8:1179–1187. [PubMed: 17952043]
- Scheurwater E, Reid CW, Clarke AJ. Lytic transglycosylases: bacterial space-making autolysins. *Int J Biochem Cell Biol*. 2008; 40:586–591. [PubMed: 17468031]
- Segal G, Shuman HA. Characterization of a new region required for macrophage killing by *Legionella pneumophila*. *Infect Immun*. 1997; 65:5057–5066. [PubMed: 9393796]
- Segal G, Purcell M, Shuman HA. Host cell killing and bacterial conjugation require overlapping sets of genes within a 22-kb region of the *Legionella pneumophila* genome. *Proc Natl Acad Sci U S A*. 1998; 95:1669–1674. [PubMed: 9465074]
- Shin S, Case CL, Archer KA, Nogueira CV, Kobayashi KS, et al. Type IV secretion-dependent activation of host MAP kinases induces an increased proinflammatory cytokine response to *Legionella pneumophila*. *PLoS Pathog*. 2008; 4:e1000220. [PubMed: 19043549]
- Stenbak CR, Ryu JH, Leulier F, Pili-Floury S, Parquet C, et al. Peptidoglycan molecular requirements allowing detection by the *Drosophila* immune deficiency pathway. *J Immunol*. 2004; 173:7339–7348. [PubMed: 15585858]
- Swanson MS, Isberg RR. Association of *Legionella pneumophila* with the macrophage endoplasmic reticulum. *Infect Immun*. 1995; 63:3609–3620. [PubMed: 7642298]
- Travassos LH, Carneiro LA, Girardin SE, Boneca IG, Lemos R, et al. Nod1 participates in the innate immune response to *Pseudomonas aeruginosa*. *J Biol Chem*. 2005; 280:36714–36718. [PubMed: 16150702]



- Travassos LH, Carneiro LA, Ramjeet M, Hussey S, Kim YG, et al. Nod1 and Nod2 direct autophagy by recruiting ATG16L1 to the plasma membrane at the site of bacterial entry. *Nat. Immunol.* 2010; 11:55–62. [PubMed: 19898471]
- Uehara T, Park JT. Identification of MpaA, an amidase in *Escherichia coli* that hydrolyzes the gamma-D-glutamyl-meso-diaminopimelate bond in murein peptides. *J Bacteriol.* 2003; 185:679–682. [PubMed: 12511517]
- Viala J, Chaput C, Boneca IG, Cardona A, Girardin SE, et al. Nod1 responds to peptidoglycan delivered by the *Helicobacter pylori* cag pathogenicity island. *Nat Immunol.* 2004; 5:1166–1174. [PubMed: 15489856]
- Vogel JP, Andrews HL, Wong SK, Isberg RR. Conjugative transfer by the virulence system of *Legionella pneumophila*. *Science.* 1998; 279:873–876. [PubMed: 9452389]
- Zamboni DS, Kobayashi KS, Kohlsdorf T, Ogura Y, Long EM, et al. The BirC1e cytosolic pattern-recognition receptor contributes to the detection and control of *Legionella pneumophila* infection. *Nat Immunol.* 2006; 7:318–325. [PubMed: 16444259]

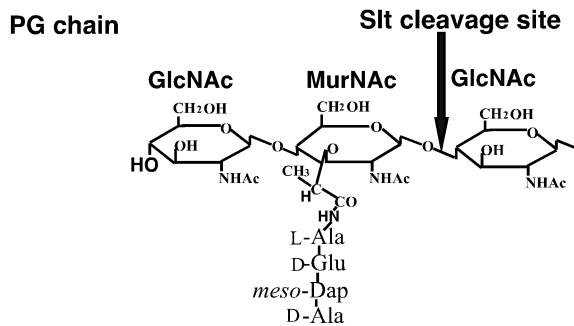
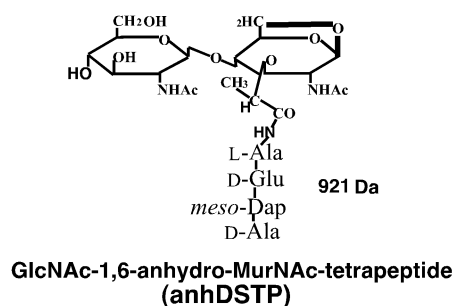
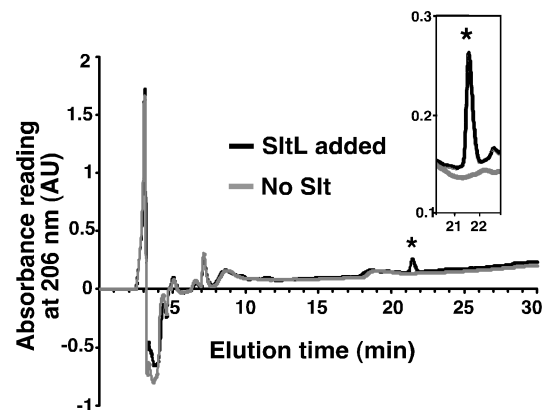
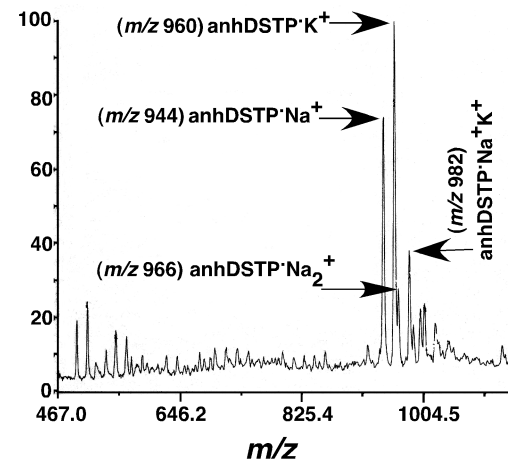
**HIGHLIGHTS**

- *L. pneumophila* EnhC directly inhibits soluble lytic peptidoglycan transglycosylase (Slt)
- SltL overexpression causes enhanced NF- $\kappa$ B activation and depressed intracellular growth
- SltL inhibition by EnhC is required to suppress Nod1-dependent NF- $\kappa$ B activation
- Growth of the *L. pneumophila*  $\Delta$ enhC strain is rescued in Nod1 deficient macrophages



**Figure 1. *L. pneumophila* EnhC directly binds *L. pneumophila* soluble lytic peptidoglycan transglycosylase (SltL)**

(A) SltL specifically binds EnhC-coated beads. Lysates of *L. pneumophila* were incubated with EnhC-Affigel beads. Bound proteins were released from the beads by boiling in SDS, separated by 10 % SDS-PAGE and visualized by silver staining (Experimental Procedures). Left lane: *L. pneumophila* extract incubated with control Affigel; Middle lane: *L. pneumophila* extracts incubated with EnhC-Affigel; Right lane: boiled beads from buffer incubated with Affigel-EnhC. (B) EnhC directly binds SltL. GST-SltL- or GST-Glutathione-Sepharose beads were incubated with purified EnhC and proteins associated with the beads were analyzed by Western blot using anti-EnhC. T: Total input of EnhC; B: EnhC bound to beads; S: EnhC in the supernatant after incubation with beads. (C) EnhC binds *L. pneumophila* Slt (SltL) with higher affinity than *E. coli* Slt (SltE). ELISA plates coated with SltL or SltE or BSA were probed with increasing concentrations of EnhC. Shown are mean  $\pm$  standard deviation (s.d.) of triplicate wells. The experiment was repeated 3 times. (D). High affinity binding of SltL is maintained at pH = 4.5. Experiment performed exactly as in panel C, probing wells coated with proteins noted in the legend. See also Fig. S1.

**A****Product****B****C**

**Figure 2. Transglycosylation of *L. pneumophila* peptidoglycan (PG) by SltL**  
 (A) Slt cleaves the  $\beta$ -1,4-glycosidic bond between MurNAc and GlcNAc in the glycan strand and generates an intramolecular 1,6-anhydro linkage between the C1 and C6 positions in the sugar ring of MurNAc, releasing GlcNAc-1,6-anhydro-MurNAc-tetrapeptide (MW = 921Da). (B) Identification of a product generated by SltL incubation with PG. *L. pneumophila* PG was incubated with SltL and subjected to HPLC (black line). The elution time of purified GlcNAc-1,6-anhydro-MurNAc-tetrapeptide (anhDSTP) is indicated by the asterisk and overlaps with the SltL product (inserted image). (C) Peak in 2(B) was subjected to MALDI-TOF mass spectrometry. Four forms of modified anhDSTP were identified.

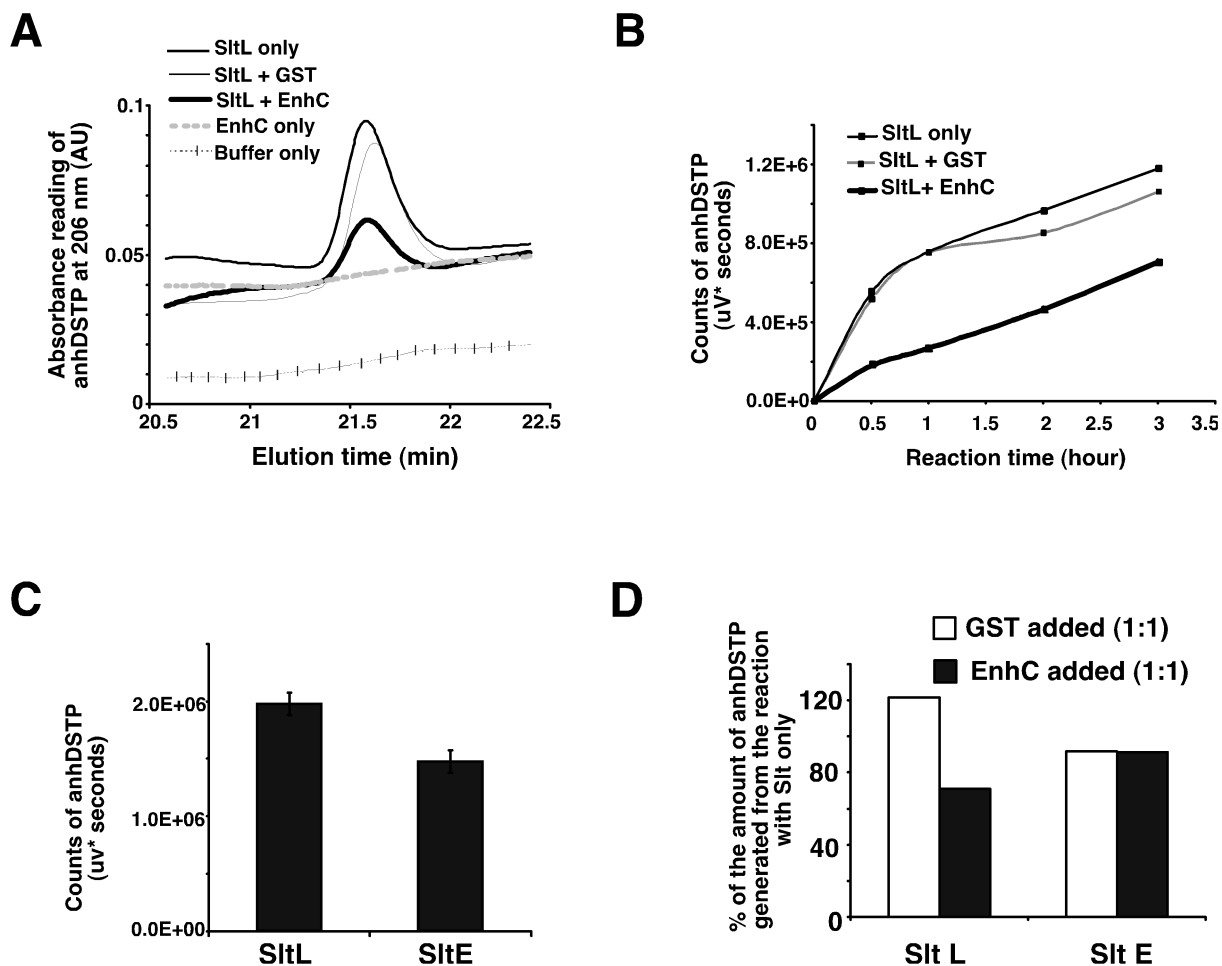


**Figure 3. EnhC specifically inhibits the enzymatic activity of *L. pneumophila* SltL**

(A) EnhC interferes with SltL activity. Equimolar amounts of EnhC and SltL were incubated with *L. pneumophila* PG at pH = 4.5 and production of anhdDSTP was monitored by HPLC fractionation. (B) EnhC causes severe reduction in the level of anhdDSTP produced by SltL. EnhC or GST was added to SltL in equimolar amounts and the production of anhdDSTP was followed over time. (C) *E. coli* SltE cleaves *L. pneumophila* PG. SltE was incubated with *L. pneumophila* PG for 16 hr and the amount of anhdDSTP was quantified based on the HPLC elution peak of anhdDSTP. Means  $\pm$  s.d. from triplicate reactions are shown. (D) EnhC does not interfere with SltE activity. Displayed is the amount of SltE activity in the presence of EnhC compared to its absence. Production of anhdDSTP was determined as in panel A. Data represent the mean value from two independent reactions for a typical experiment. See also Fig. S2.



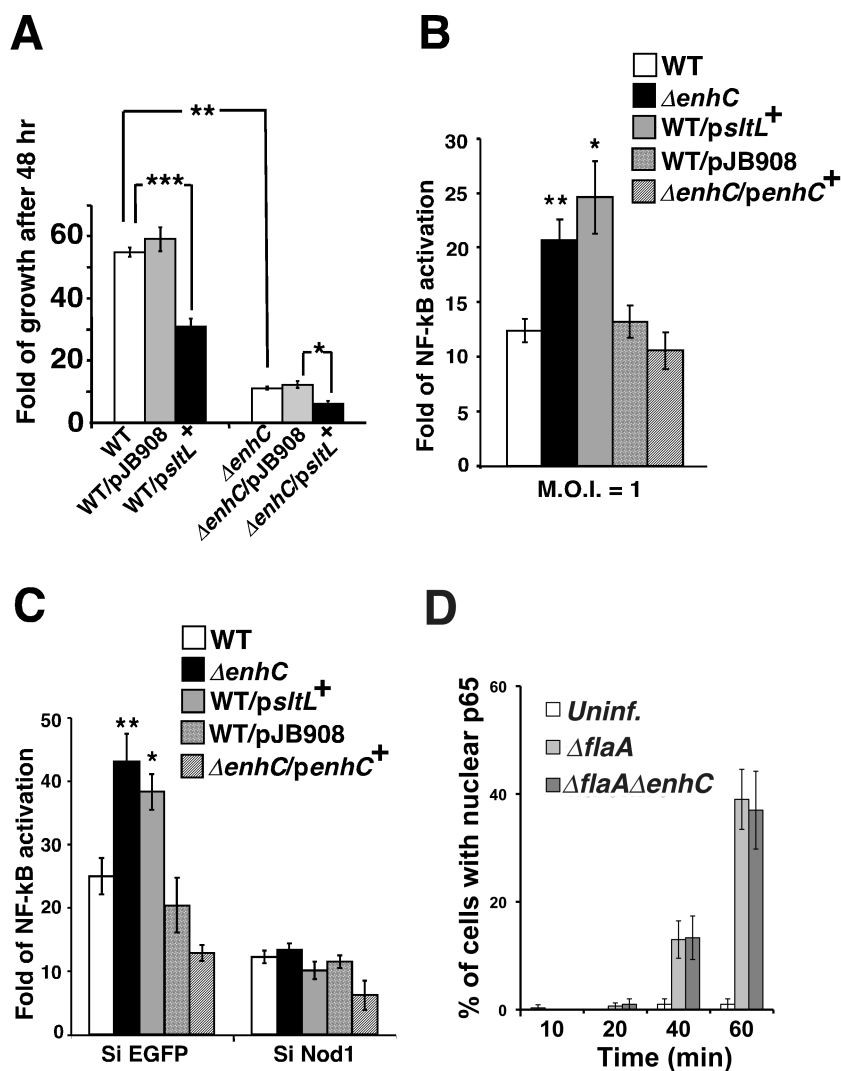


**Figure 4. Overexpression of SltL results in aberrant Nod1-dependent NF- $\kappa$ B activation and defective intracellular growth in host cells**

(A) Overexpression of SltL is detrimental to the intracellular growth of *L. pneumophila* in mouse bone marrow derived macrophages (BMDMs). Fold growth = (CFU at 48 hr post-infection)/(CFU at 2 hr post-infection). WT: *L. pneumophila* LP02;  $\Delta$ enhC: MLL101; WT/psltL<sup>+</sup>: MLL801;  $\Delta$ enhC/psltL<sup>+</sup>: MLL901; pJB908: empty vector. \*\*\*:  $P < 0.0005$ ; \*\*:  $P < 8.17E-06$ ; \*:  $P < 0.005$ . (B) Overexpression of SltL stimulates NF- $\kappa$ B activation in HEK293T cells challenged by *L. pneumophila*.  $\Delta$ enhC/penhC<sup>+</sup>: MLL201. NF- $\kappa$ B activation was measured using luciferase fused to NF- $\kappa$ B sensitive promoter (Experimental Procedures). Data are represented as luciferase units from infected samples/ luciferase units in uninfected controls. \*\*:  $P < 0.003$ ; \*:  $P < 0.003$ . (C) Overexpression of SltL causes Nod1-dependent NF- $\kappa$ B activation. NF- $\kappa$ B activation was measured as above in HEK293T cells depleted of Nod1 (SiNod1) or with control (SiEGFP). Fold activation = luciferase units from infected samples/ luciferase units of uninfected sample. \*\*:  $P < 0.002$ ; \*:  $P < 0.004$ . See also Fig. S3. (D) Time course of p65 translocation. Bone marrow macrophages from C57BL/6 *myd88*<sup>-/-</sup> mice were challenged with noted bacterial strains at MOI = 1 and NF- $\kappa$ B p65 nuclear localization was determined (Losick and Isberg 2006). For panels A and D, mean +/-

– s.d. from 3 samples are shown. For panel B and C, means  $\pm$  s.d. from 6 samples are shown. *P* value was calculated by unpaired two-tailed Student's *t*-test.

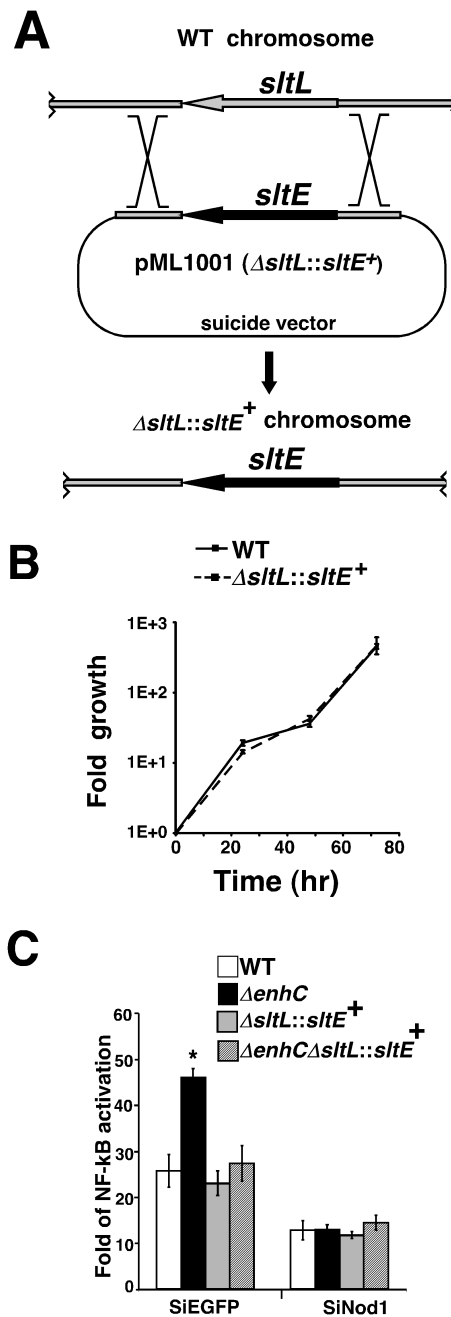


**Figure 5. The  $\Delta enhC$  phenotype requires SltL function**

(A) Construction of *L. pneumophila* strain with *sltL* replaced by *sltE* (MLL1001;  $\Delta sltL::sltE^+$ ). A DNA fragment containing the ORF of *sltE* flanked by *L. pneumophila* chromosomal DNA was cloned into suicide vector pSR47S. Selection for integration and recombination is as described (Experimental Procedures). (B) MLL1001 ( $\Delta sltL::sltE^+$ ) grows as well as WT in mouse bone marrow derived macrophages (BMDMs). The intracellular growth of *L. pneumophila* was monitored by measuring CFU every 24 hr during a 3 day incubation (Experimental Procedures). (C) Replacement of *sltL* with *sltE* bypasses the  $\Delta enhC$  defect. NF- $\kappa$ B activation was determined by luciferase reporter assay. WT: LP02.  $\Delta enhC$ : MLL101.  $\Delta sltL::sltE^+$ : MLL1001.  $\Delta enhC \Delta sltL::sltE^+$ : MLL1101. \*: *P*

< 0.001. For panel B and C, a representative experiment is shown; experiment was repeated 3 times. For panel B, means  $\pm$  s.d. from 3 samples are shown. For panel C, means  $\pm$  s.d. from 6 samples are shown. *P* value was calculated by unpaired two-tailed Student's *t*-test. See also Fig. S4

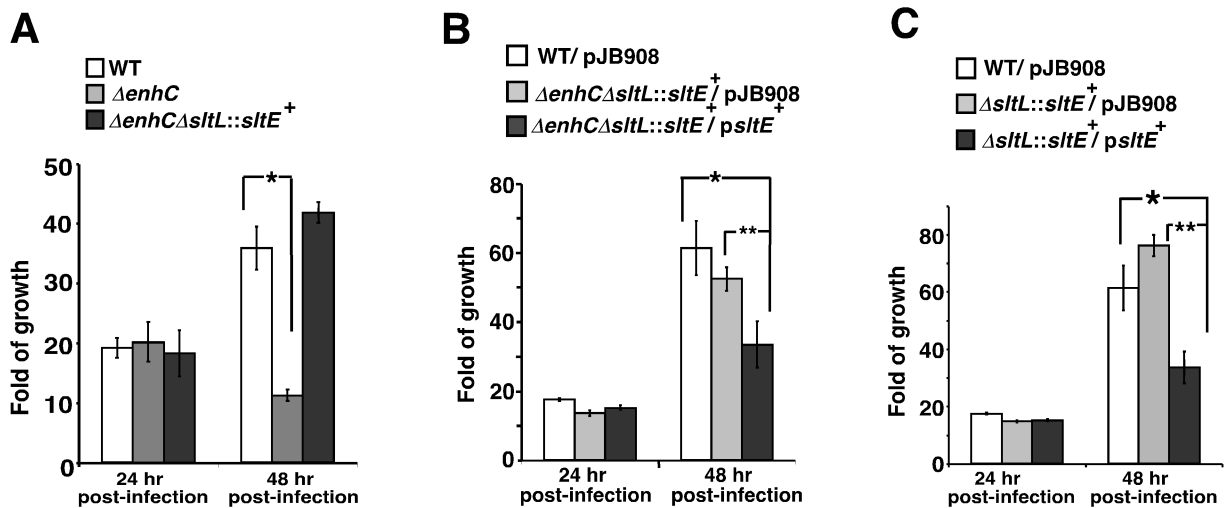


**Figure 6. The inhibition of SltL by EnhC promotes intracellular growth of *L. pneumophila***  
 (A) Replacement of *sltL* bypasses the  $\Delta enhC$  defect for intracellular growth. WT: LP02;  $\Delta enhC$ : MLL101;  $\Delta enhC \Delta sltL::sltE^+$ : MLL1101. \*:  $P < 0.003$ . (B) Overexpression of SltE in the absence of EnhC and SltL causes an intracellular growth defect. pJB908: empty vector. WT/pJB908: MLL221;  $\Delta enhC \Delta sltL::sltE^+/pJB908$ : MLL1101/pJB908;  $\Delta enhC \Delta sltL::sltE^+/psltE^+$ : MLL1301. \*:  $P < 0.01$ ; \*\*:  $P < 0.012$ . (C) Overexpression of SltE in the presence of EnhC causes an intracellular growth defect.  $\Delta sltL::sltE^+/pJB908$ : MLL 1001/pJB908;  $\Delta sltL::sltE^+/psltE^+$ : MLL1201. \*:  $P < 0.008$ ; \*\*:  $P < 0.0004$ . For all panels, a representative experiment is shown and the experiments were repeated 3 times. Means  $\pm$  s.d. from triplicate samples are shown.  $P$  value was calculated by unpaired two-tailed Student's  $t$ -test.



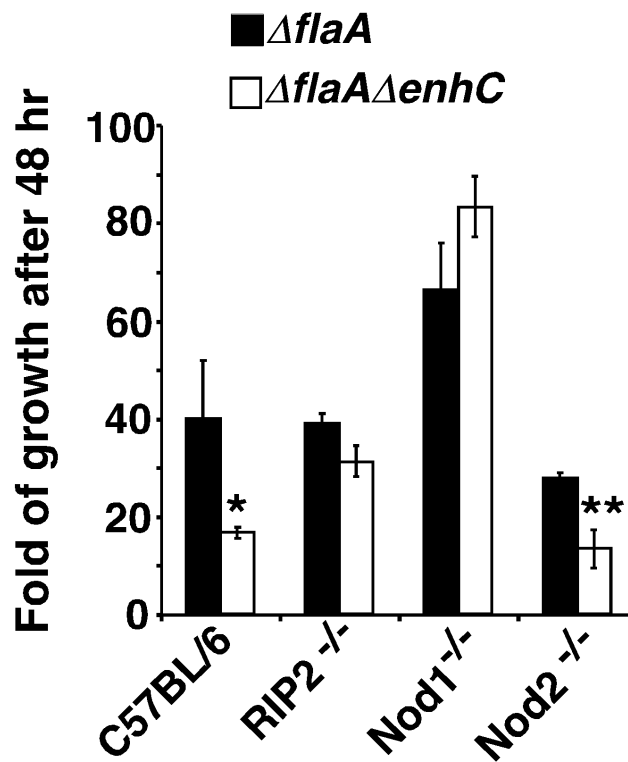


**Figure 7. The absence of Nod1 allows proficient growth of the  $\Delta enhC$  strain**  
 C57BL/6J bone marrow derived macrophages from the indicated knockout mice were challenged with *L. pneumophila* and intracellular growth was determined by plating for CFU after 48 hrs incubation.  $\Delta flaA$  strains were used to prevent the Naip5/Birc1e signaling that occurs in the C57BL/6 mouse background.  $\Delta flaA$ : MLL099;  $\Delta flaA \Delta enhC$ : MLL111. \*\*:  $P < 0.001$ ; \*:  $P < 0.03$ . A representative experiment is shown and the experiment was repeated 3 times. Data are expressed as mean  $\pm$  s.d. from triplicate samples.  $P$  value was calculated by unpaired two-tailed Student's  $t$ -test. See also Fig. S5.

**Table 1**

## Bacterial strains and plasmids used in this work

Strain/plasmid	Genotype/ relevant characteristics	Reference
pSR47s oriTRP4	<i>oriT<sub>RP4</sub> oriP<sub>R6k</sub> sacB</i> Kan <sup>R</sup> suicide vector	(Rankin et al. 2002)
pJB908	pMMB66EH <i>oriP<sub>RSF1010</sub> ΔoriT bla<sup>+</sup> tdΔI</i>	(Laguna et al. 2006)
pKB5	pMMB66EH <i>oriP<sub>RSF1010</sub> tdΔI bla<sup>+</sup></i>	(Berger and Isberg 1993)
pGE148	pQE-32-His-tagged EnhC	(Liu et al. 2008)
pML701	pGEX-6P-1-GST-tagged <i>L. pneumophila</i>	Slt this study
pMLD204	pET-His-tagged <i>E. coli</i> Slt	(Stenbak et al. 2004)
pML101	pSR47s <i>ΔenhC</i>	(Liu et al. 2008)
pML201	pJB908 <i>enhC</i> <sup>+</sup>	(Liu et al. 2008)
pML301	pSR47s <i>ΔsltL</i>	this study
pML601	pKB5 <i>sltL</i> <sup>+</sup>	this study
pML801	pJB908 <i>sltL</i> <sup>+</sup>	this study
pML1001	pSR47s <i>ΔsltL :: sltE</i> <sup>+</sup>	this study
pML1201	pJB908 <i>sltE</i> <sup>+</sup>	this study
LP02	Philadelphia-1 <i>rpsL hsdR thyA</i> <sup>-</sup>	(Berger and Isberg 1993)
LP03	LP02 <i>dotA03</i>	(Berger et al. 1994)
MLL099	LP02 <i>ΔflaA</i>	(Ren et al. 2006)
MLL101	LP02 <i>ΔenhC</i>	(Liu et al. 2008)
MLL111	LP02 <i>ΔflaAΔenhC</i>	this study
MLL201	LP02 <i>ΔenhC</i> /pML201	(Liu et al. 2008)
MLL211	LP02 <i>ΔenhC</i> /pJB908	(Liu et al. 2008)
MLL221	LP02/pJB908	(Liu et al. 2008)
MLL301	LP02 <i>ΔsltL</i>	this study
MLL601	LP02 <i>ΔsltL</i> / pML601	this study
MLL611	LP02 <i>ΔsltL</i> / pKB5	this study
MLL801	LP02/pML801	this study
MLL901	LP02 <i>ΔenhC</i> /pML801	this study
MLL1001	LP02 <i>ΔsltL :: sltE</i> <sup>+</sup>	this study
MLL1001/pJB908	LP02 <i>ΔsltL :: sltE</i> <sup>+</sup> /pJB908	this study
MLL1101	LP02 <i>ΔenhC ΔsltL :: sltE</i> <sup>+</sup>	this study
MLL1101/pJB908	LP02 <i>ΔenhC ΔsltL :: sltE</i> <sup>+</sup> /pJB908	this study
MLL1201	LP02 <i>ΔsltL :: sltE</i> <sup>+</sup> /pML1201	this study
MLL1301	LP02 <i>ΔenhC ΔsltL :: sltE</i> <sup>+</sup> /pML1201	this study